Accelerated Publications

LytG of *Bacillus subtilis* Is a Novel Peptidoglycan Hydrolase: The Major Active Glucosaminidase†

Gavin J. Horsburgh, Abdelmadjid Atrih, Michael P. Williamson, and Simon J. Foster*

Department of Molecular Biology and Biotechnology, University of Sheffield, Sheffield, S10 2TN, United Kingdom

Received July 29, 2002; Revised Manuscript Received October 21, 2002

ABSTRACT: LytG (YubE) of *Bacillus subtilis* is a novel 32 kDa autolysin produced during vegetative growth under the control of Eσ^A RNA polymerase. Muropeptide analysis of vegetative cells of *B. subtilis* revealed LytG to be the major glucosaminidase responsible for peptidoglycan structural determination during vegetative growth. Overexpression and purification of LytG allowed its biochemical characterization. Despite sequence homology suggesting muramidase activity, LytG is a novel glucosaminidase with exoenzyme activity and may form part of a novel family of autolysins. It is involved in cell division, lysis, and motility on swarm plates.

Peptidoglycan is essential for the maintenance of cellular viability and shape determination for most eubacteria. It is a dynamic structure continually being synthesized, modified, and hydrolyzed to allow for cell growth and division. Bacteria produce a complement of autolysins capable of hydrolyzing the peptidoglycan structure of their own cell wall (*1*). These autolysins have been implicated in several important cellular functions, including differentiation, cell lysis, cell wall growth and turnover, cell separation, competence, motility, and antibiotic-induced lysis (*2*−*6*). *Bacillus subtilis* 168 has two major autolysins expressed during the vegetative phase of growth, a 50 kDa *N*-acetylmuramyl-L-alanine amidase (LytC) and a 90 kDa *N*-acetylglucosaminidase (LytD) (*7*, *8*). Both enzymes are dispensable for growth but have often mutually compensatory roles in cell wall turnover, motility, and cell separation (*9*−*13*). Expression of *lytC* and *lytD* is mainly under the control of the sigma factor, σ^D,[1] which controls the flagellar, chemotaxis and motility regulon (*12*, *14*, *15*).

As well as the discovery of the endo-β-*N*-acetylglucosaminidase (LytD) in *B. subtilis* 168 an exo-β-*N*-acetylglucosaminidase has been characterized from *B. subtilis* B (*16*−*19*). This exo-β-*N*-acetylglucosaminidase has a molecular weight of about 75 kDa and an optimum pH of 5.9. A mutant lacking the exo-β-*N*-acetylglucosaminidase showed no change in growth, division or sporulation (*20*). Although Ortiz et al. (*19*) suggest the production of a similar exo-β-*N*-acetylglucosaminidase at low levels in *B. subtilis* 168, no further evidence of its existence has been shown.

Renaturing SDS−PAGE analysis and the genome sequence of *B. subtilis* have revealed the presence of multiple putative novel autolysins, which have begun to be characterized (*21*−*25*). The complex compensatory nature of the autolysins means that it is important to identify and analyze the total complement of these enzymes to determine their individual and combined roles. One of the putative novel autolysins identified by sequence homology is a 32kDa possible muramidase (*25*), encoded by the *lytG* (formerly *yubE*) gene, and shows greatest homology to the autolysins AcmA of *Lactococcus lactis* and AlyS of *Enterococcus hirae*. The *lytG* gene is situated in a possible bi-cistronic operon with the downstream gene *yubF*, which encodes a putative protein of unknown function. In this study, we have characterized LytG as a novel exoglucosaminidase with a role during vegetative growth.

EXPERIMENTAL PROCEDURES

Bacterial Strains, Plasmids, and Growth Conditions. All *B. subtilis* strains and plasmids used in this study are shown in Table 1. Unless otherwise stated *B. subtilis* strains were grown in nutrient broth (Oxoid) at 37 °C with shaking (250 rpm) or on nutrient agar plates at 37 °C. Plasmids were constructed in, and prepared from, *Escherichia coli* strain DH5α grown in Luria-Bertani (LB) broth or on LB agar at 37 °C. When appropriate, chromosomal drug resistance markers in *B. subtilis* were selected with kanamycin (10 μg mL^{-1}), erythromycin (1 μg mL^{-1}), lincomycin (25 μg mL^{-1}), spectinomycin (100 μg mL^{-1}), phleomycin (0.3 μg mL^{-1}),

† This research was funded by the BBSRC and the Royal Society.

* Corresponding author. Mailing address: Department of Molecular Biology and Biotechnology, University of Sheffield, Firth Court, Western Bank, Sheffield, S10 2TN, United Kingdom. Phone: 44 114 222 4411. Fax: 44 114 272 8697. E-mail: s.foster@sheffield.ac.uk.

[1] Abbreviations, RP-HPLC, reverse phase high-pressure liquid chromatography; σ, sigma factor; COSY, correlated spectroscopy; TOCSY, total correlated spectroscopy; ROESY, rotating frame nuclear Overhauser effect spectroscopy; EDTA, ethylenediaminetetraacetic acid; WT, wild type; CWBP, cell wall binding protein; MurNAc, *N*-acetylmuramic acid; GlcNAc, *N*-acetylglucosamine; A_2pm, *meso*-diaminopimelic acid.

10.1021/bi020498c CCC: $25.00
Published on Web 12/19/2002

Table 1: Bacterial Strains and Plasmids

strain or plasmid	genotype/phenotype	source/ref[a]
	Strains	
B. subtilis 168		
1A304	*trpC2 metB5 xin-1 SPβ*(s)	BGSC[b]
GJH100	*trpC2 metB5 xin-1 SPβ*(s) *lytG*::pMUTIN4, Em^r	this study
SH115	*trpC2 metB5 xin-1 SPβ*(s) *lytC*::*ble*	*13*
SH119	*trpC2 metB5 xin-1 SPβ*(s) *lytD*::*spc*	*13*
SH118	*trpC2 metB5 xin-1 SPβ*(s) *sigD*::pLM5 Cm^r	*13*
SH128	*trpC2 metB5 xin-1 SPβ*(s) *lytC*::*ble lytD*::*spc*	*13*
SH131	*trpC2 metB5 xin-1 SPβ*(s) *lytC*::*ble lytD*::*spc sigD*::pLM5 Cm^r	*13*
GJH104	*trpC2 metB5 xin-1 SPβ*(s) *lytG*::pMUTIN4, Em^r *lytC*::*ble*	GJH100 > SH115
GJH144	*trpC2 metB5 xin-1 SPβ*(s) *lytG*::pMUTIN4, Em^r *lytD*::*spc*	GJH100 > SH119
GJH110	*trpC2 metB5 xin-1 SPβ*(s) *lytG*::pMUTIN4, Em^r *lytC*::*ble lytD*::*spc*	GJH100 > SH128
GJH113	*trpC2 metB5 xin-1 SPβ*(s) lytG::pMUTIN4, Em^r *lytC*::*ble lytD*::*spc sigD*::pLM5 Cm^r	GJH110 > SH118
GJH145	*trpC2 metB5 xin-1 SPβ(s) yubF*::*kan*	this study
GJH146	*trpC2 metB5 xin-1 SPβ(s) yubF*::*kan lytC*::*ble*	GJH145 > SH115
GJH147	*trpC2 metB5 xin-1 SPβ(s) yubF*::*kan lytC*::*ble lytD*::*spc*	GJH145 > SH128
E. coli		
DH5α	*supE44*Δ lacU169 (Φ80 *lacZ* Δ*M15*) *hsdR17 recA1 endA1 gyrA96 thi-1 relA1*	*30*
BL21(DE3)	F-*ompT hsdS*$_B$($r_B^- m_B^-$) *gal dcm* (DE3)	Novagen
	Plasmids	
pMUTIN4	insertion vector, Erm^r	*27*
pUC119	cloning vector, Ap^r	laboratory stocks
pGJH121	pUC119 with 2.25 kb *Bam*HI-*Sac*I fragment containing *yubF* gene with an engineered *Xho*I site	this study
pGJHy2k	pUC119 with 2.25 kb *Bam*HI-*Sac*I fragment containing *yubF* gene with a kanamycin cassette inserted in the engineered *Xho*I site	this study
pGJH100	pMUTIN4 containing a 300 bp *Hin*dIII-*Bam*HI insert carrying part of the *yubE* gene	this study
pETGJH6	pET24d containing *lytG* gene with its signal sequence removed and C-terminal His tag added	this study

[a] Arrows (>) indicate transformation of recipient strain with donor chromosomal DNA. [b] *Bacillus* Genetic Stock Center, Ohio State University, Columbus, OH.

or chloramphenicol (5 μg mL^{-1}). In *E. coli*, plasmids were selected with ampicillin (50 μg mL^{-1}).

Construction of Mutants Insertionally Inactivated in lytG and yubF. (i) Plasmid Construction. Nucleotide sequence from the *B. subtilis* complete genome sequence (*26*) was used to clone an internal fragment of the *lytG* gene into pMUTIN4 (27) to create plasmid pGJH100. Using genomic DNA as a template a 300 bp fragment was amplified by PCR using the forward primer (5'-GCCGAAGCTT$_{64}$*CCGCTAGCTC-TGTTTGTTT*$_{83}$) and the reverse primer (5'-CGCGGATCC$_{368}$ *CGAATGGTTTTTCTTTTCC*$_{349}$), where the restriction sites are underlined and the internal sequence of the gene is italicized (numbering is with respect to the A of the translational start codon of the gene). Nucleotide sequence from the *B. subtilis* complete genome sequence (*26*) was used to amplify, by PCR, two fragments either side of the *yubF* gene and overlapping. One stretching from 982 bp before the start of, to 50 bp into the *yubF* gene was amplified using the forward primer (5'-CGCGCGGATCC*CGAAGGAAG-GTT*$_{-958}$) and the reverse primer (5'-*TAAGCTAGTACT*CTC-GA*GCAACCGTGTTTCTGCGTC*$_{13}$). The other fragment stretches from 50 bp in, to 1002 bp after the end of, the gene and was amplified using the forward primer (5'-*GACGCAGAAACACGGTTGCCTCGAGAGTACTAGCT-TA*$_{50}$) and the reverse primer (5'-GCGAGCTC*GCCGACA-ATCGGCGG*$_{1002}$). The two fragments were placed in a PCR reaction with the two external primers to amplify the whole region. The product was cleaned by gel extraction and digested with *Bam*HI and *Sac*I alongside pUC119. The digested products were ligated by the method of Sambrook et al. (*28*). The resultant plasmid pGJH170 was digested with *Xho*I that cuts the ligated fragment at the engineered site and also 33 bp into the *yubF* gene. A kanamycin cassette was excised from pDG782 (29) by digestion with *Xho*I and *Sal*I and then ligated with pGJH170. The resultant plasmid, pGJHy2k, therefore contained the *yubF* gene inactivated by the insertion of a kanamycin cassette. Multiple mutant strains were made by transformation with the appropriate chromosomal DNA (Table 1).

(ii) Transformation of E. coli and B. subtilis. Transformation of *E. coli* was performed as described by Hanahan (*30*). Transformation of *B. subtilis* 168 with pGJH100 and pGJHy2k was performed by the competent cell method (*31*). Confirmation of *lytG* gene disruption by means of Campbell-type recombination was achieved by Southern blot analysis, using pMUTIN4 *Hpa*I digested fragment containing the multiple cloning site as a probe. Southern blot analysis, using the *yubF* containing 2.25 kbp fragment from pGJH170 as a probe, showed that the kanamycin resistance cassette had been inserted into the *yubF* gene by a double crossover event creating the strain GJH145. Hybridization, probe labeling, and detection were done using the Boehringer Mannheim nonradioactive DNA labeling and detection kit.

Analysis of Gene Expression. To measure gene expression during sporulation, synchronous sporulation was performed using the resuspension method of Sterlini & Mandelstam (*32*). After the initiation of sporulation (t_0), samples were harvested every hour for 9 h and sporulation morphology monitored by microscopy. Levels of β-galactosidase activity were measured as described by Horsburgh and Moir (*33*).

Cell Separation. The measurement of filamentation and macrofilamentation was performed as described by Blackman et al. (*13*), with the exception of shaking at 40 rpm instead of 45 rpm for liquid cultures grown at 25 °C.

Swarm Plate Assay. Swarming motility of strains was measured on nutrient agar plates (0.3% w/v) as described by Blackman et al. (*13*).

Cell Autolysis and Preparation of Cell-Wall-Binding Protein (CWBP) Extracts. Lysis of cells of *B. subtilis* parental and mutant was performed and cell wall binding proteins prepared as described by Blackman et al., (*13*).

Overexpression and Purification of LytG Protein. Nucleotide sequence from the *B. subtilis* complete genome sequence (*26*) was used to amplify the *lytG* gene with both its putative signal sequence and stop codon removed. The 801 bp fragment of *lytG* was amplified using the forward primer (5'-GTTTCCATGG*CAACTTTATCAAAACCGATTGA*$_{110}$) and the reverse primer (5'-TAAACTCGAG*GGTTGCCTCCTTTATTTCA*$_{827}$). The fragment was cleaned by gel extraction and restricted with *Xho*I and *Nco*I alongside pET24d. The restricted products were ligated using the method of Sambrook et al. (*28*), creating the plasmid pETGJH6. Transformation of *E. coli* BL21(DE3) with pGJH6 was as described by Hanahan (*30*). The cloned *lytG* gene was sequenced which determined that no errors in its sequence had occurred during amplification (results not shown). Cultures of BL21(DE3) containing pETGJH6 in LB + glucose (0.5% w/v) + Kanamycin (30 μg mL^{-1}) were grown overnight (25 °C, 250 r.p.m) and inoculated 1 in 20 into LB with glucose and kanamycin. Cells were grown at 25 °C, 250 rpm until OD_{600} reached 0.6−0.8 at which point (IPTG) was added to a final concentration of 0.4 mM. Samples were taken before the addition of IPTG and at hourly intervals for 4 h for SDS−PAGE and renaturing SDS−PAGE analysis. Cells were harvested at 4 h and sonicated, and His-tagged LytG protein was purified using HisTrap metal chelate affinity chromatography as described in the manufacturers instructions (Amersham Pharmacia Biotech, U.K.).

SDS−PAGE and Renaturing SDS−PAGE. Protein samples from overexpression studies and CWBP samples were analyzed by 12% (w/v) SDS−PAGE (*34*) and Coomassie blue staining to visualize proteins. Renaturing gel electrophoresis using purified *B. subtilis* vegetative cell walls as substrate was used to detect autolysin activity as described by Foster (*21*).

Analysis of LytG Activity. All assays were carried out at 37 °C in a Victor^2 (Wallac), in 96 well plates with *B. subtilis* cell walls (0.19 mg mL^{-1}) and purified LytG (20 μg mL^{-1}). Activity was measured as loss of OD_{450}, with 1 unit of enzyme activity being defined as that, which will result in loss of 0.001 OD_{450} units/min^{-1}. To determine the optimum pH, buffer and cation for LytG activity sodium citrate, phosphate, and Tris/HCl buffers with pH's ranging from 3 to 6.3, 5.8 to 8.0, and 7 to 9, respectively were used. The presence of 20mM of the cations, $MgCl_2$, $CaCl_2$, $CuCl_2$, $HgCl_2$, or $ZnCl_2$, the chelator EDTA, or a range of $MgCl_2$ and $CaCl_2$ concentrations (0−100mM) were also tested.

Analysis of lytG Promoters. Primer extension was carried out as described previously (*34*).

Analysis of Enzymatic Hydrolysis of Peptidoglycan by RP-HPLC. Preparation of cell wall peptidoglycan and separation of soluble muropeptides were carried out as previously described (*35*) but with the following modifications. Peptidoglycan (2 mg mL^{-1}) was hydrolyzed with purified LytG (50−200 μg mL^{-1}) at 37 °C with samples taken at defined intervals. Some samples were boiled and treated with Cellosyl as described by Atrih et al. (*36*). Before purification, samples were reduced using borohydride, which converts the reducing sugar to its corresponding alcohol. Muropeptides were analyzed by mass spectrometry (MS) measurements using MALDI-TOF (*36*). NMR analysis was carried out on Bruker DRX-500 and DRX-600 spectrometers. Samples were analyzed using two-dimensional correlated spectroscopy (COSY), total correlated spectroscopy (TOCSY), and rotating frame nuclear Overhauser effect spectroscopy (ROESY). For TOCSY, a spin-lock field of 9 kHz was used over a mixing time of 95 ms, while for ROESY, a spin-lock field of 3 kHz was used over a mixing time of 150 ms. Spectra were processed using FELIX (Accelrys Inc., San Diego, CA).

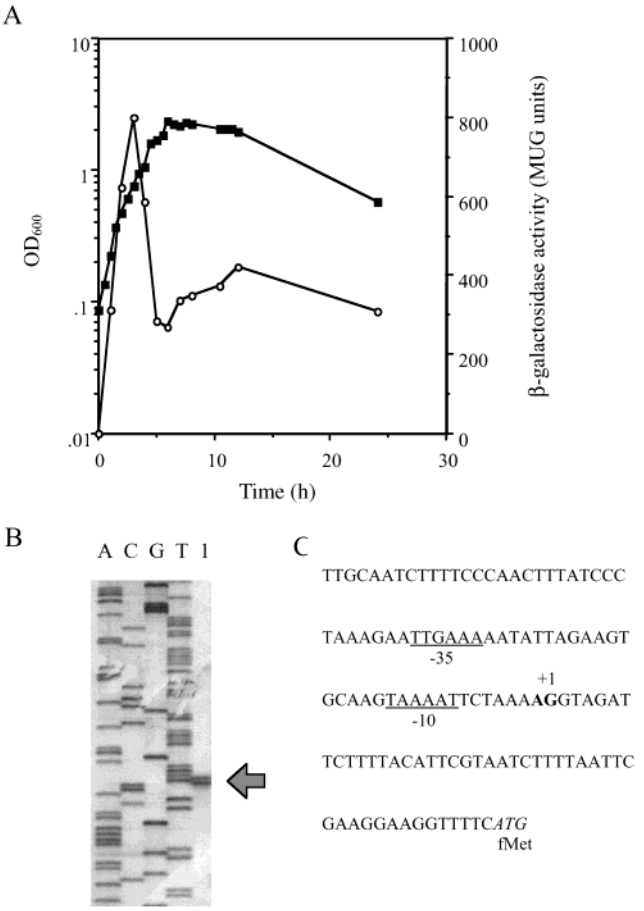

FIGURE 1: The *lytG* gene is vegetatively expressed. (A) Expression of *lytG::lacZ* was measured in GJH100 during growth in NB at 37 °C. OD_{600} (closed symbols), β-galactosidase activity (open symbols). (B) Analysis of the 5′ end of the *lytG* transcript by primer extension. The sequencing ladder is in lanes A, C, G, and T. Lane 1 is the primer extension of RNA from strain 1A304. (C) Chromosomal DNA sequence proximal to the *lytG* transcriptional start site. The transcriptional and translational starts are shown in bold and italics, respectively. The putative −10 and −35 regions are underlined.

RESULTS

Analysis of lytG Expression. Expression of *lytG* was measured using a *lacZ* reporter fusion in strain GJH100. Maximal expression was observed during the mid-exponential phase of vegetative growth (Figure 1A), with none during sporulation (results not shown). Total RNA was purified from the wild-type strain at the estimated time of maximal

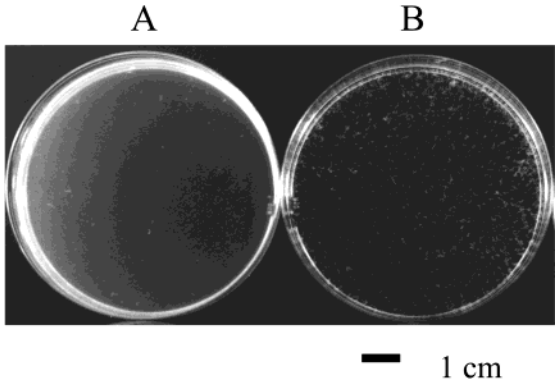

FIGURE 2: Role of autolysins in cell separation. Formation of boli in liquid cultures occurs due to the increased filamentation in strain GJH110 (*lytC lytD lytG*) mutant (B) compared to strain SH128 (*lytC lytD*) mutant (A). Liquid cultures (10 mL nutrient broth) were grown overnight at 25 °C with gentle shaking (40 rpm) and poured into Petri dishes for photography.

expression (1.5−2 h) of *lytG*. The transcriptional site for *lytG* was determined by primer extension to be located 48/49 bp upstream of the *lytG* translational start site (Figure 1B). The promoter has a −35 and −10 region of TTGAAA and TAAAAT, respectively.

Role of LytG. Cell Growth and Division. In nutrient broth (37 °C, 250 rpm) all *B. subtilis* (Table 1) strains grew at equivalent rates and reached the same final OD_{600} (results not shown). Although accurate readings could not be obtained for strains SH131(*lytC lytD sigD*) and GJH110 (*lytC lytD lytG*) due to hyperfilamentation of cells. When strains were grown at 25 °C with shaking at 40 rpm clumps of cells (boli) became visible in the medium in strain GJH110 (*lytC lytD lytG*) but not in strain SH128 (*lytC lytD*) (Figure 2). However, SH115 (*lytC*), SH119 (*lytD*), and GJH100 (*lytG*) showed no such degree of boli formation. After growth at 25 °C, 40 rpm, strains GJH110 (*lytC lytD lytG*) and SH128 (*lytC lytD*) were both observed to be highly filamentous by microscopy.

Swarming Motility. Strains SH115 (*lytC*),GJH100 (*lytG*), and GJH104 *(lytC lytG*) were motile in stationary phase when viewed by phase-contrast microscopy. These strains were analyzed on swarm plates, which measures chemotaxis as well as bacterial motility. Motile strains form a halo of diffuse growth round a tightly packed central colony on swarm plates. Strain SH115 (*lytC*) showed a reduction in swarming motility compared to its parent 1A304, the halo diameter being 44 (SD ± 0.7) versus 74 (SD ± 0.5) mm. This result is consistent with the findings of Blackman et al. (*13*). Strain GJH100 (*lytG*) also showed a reduction in swarming motility, the halo diameter being 48 (SD ± 1.3) mm. GJH104 (*lytC lytG*) demonstrated an even greater reduction in swarming (32 (SD ± 0.4) mm). No swarming motility defect was noted for strain GJH145 (*yubF*). SH128 (*lytC lytD*) and GJH110 (*lytC lytD lytG*) do not swarm at all (as previously noted for SH128 (*lytC lytD*); 13).

Cell Autolysis. Inactivation of *lytG* (strain GJH100) alone had no significant effect on lysis by cloxacillin (results not shown). Also, in combination with LytC, there was no defect over and above LytC. However, although SH119 (*lytD*) only showed a modest reduction in lysis rate in the presence of cloxacillin compared to 1A304 (79% vs 90% lysis after 90 min treatment, respectively), in GJH144 (*lytG lytD*) the effect

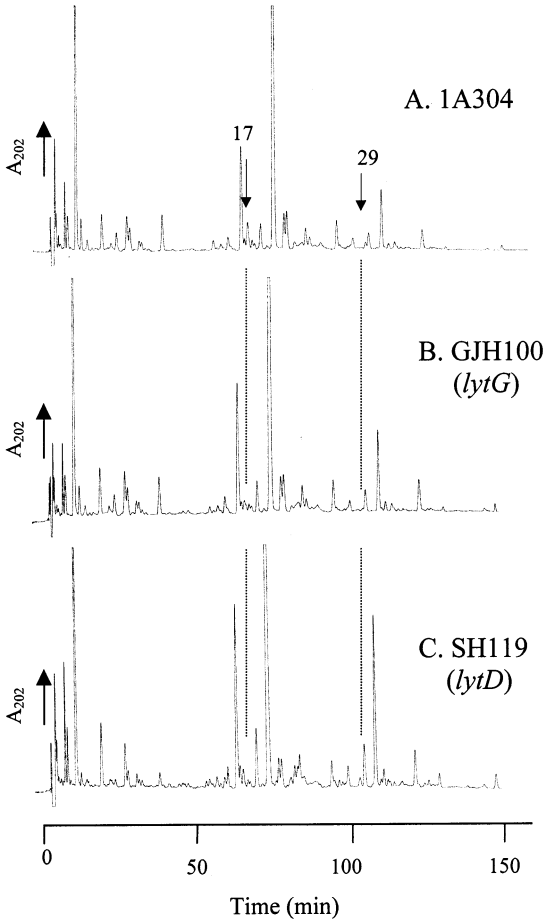

FIGURE 3: Role of LytD and LytG in *B. subtilis* peptidoglycan structural determination. RP-HPLC muropeptide elution patterns of peptidoglycan from *B. subtilis* 168 vegetative cells of 1A304 (wild type) (A), GJH100 (*lytG*) (B), and SH119 (*lytD*) (C).

was exacerbated (16% lysis after 90 min treatment). A similar compensatory role for LytD and LytG in lysis in response to sodium azide was also noted (results not shown).

Role of LytG in in Vivo Peptidoglycan Structural Determination. B. subtilis has a characteristic muropeptide profile during vegetative growth (Figure 3A) (*35*). Analysis by RP-HPLC of purified cell walls of wild type, strain SH119 (*lytD*), and strain GJH100 (*lytG*) showed a substantial reduction in muropeptide 17 and a complete loss of muropeptide 29 (see Figure 3; muropeptide designation from ref *35*). Muropeptide 17 was previously shown to contain two products named 17a and 17b, corresponding to disaccharide tripeptide disaccharide tetrapeptide with 1 phosphate and two amidations and disaccharide tripeptide disaccharide tetrapeptide with two amidations and missing a glucosamine (*35*). Muropeptide 29 was also previously identified as disaccharide tripeptide disaccharide tetrapeptide disaccharide tetrapeptide missing a glucosamine (*35*). In contrast SH119 (*lytD*) (Figure 3C) showed no alteration in muropeptide profile compared to 1A304 (WT) (Figure 3A).

Analysis of Cell-Wall-Binding Protein Extracts. Renaturing SDS−PAGE analysis of cell-wall-binding protein (CWBP) extracts of wild type and mutant strains revealed that LytG was not a major CWBP and that its action could not be demonstrated on zymograms from whole cell extracts (results not shown).

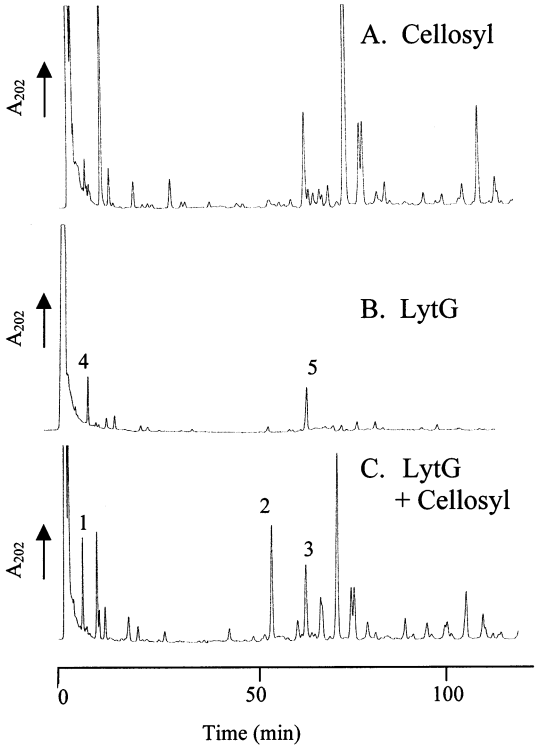

FIGURE 4: LytG has glucosaminidase activity. RP-HPLC muropeptide elution patterns of soluble peptidoglycan fragments from *B. subtilis* 168 (HR) vegetative cells hydrolyzed with: (A) Cellosyl, (B) LytG, or (C) LytG and Cellosyl.

Role of LytF. GJH145 (*yubF*) had no phenotypic differences from the wild type (1A304) in any of the above assays (results not shown).

Analysis of LytG Activity. LytG protein was overexpressed in *E. coli* and purified by virtue of a C-terminal His tag. The purified protein showed maximal activity in sodium citrate buffer (10 mM, pH 5.7). Activity was greatest in the presence of 10 mM $MgCl_2$ and was inhibited by 20 mM EDTA (results not shown). The inhibition of LytG activity by EDTA suggests that LytG was purified with chelated Mg^{2+} and that the presence of that cation is essential for LytG activity. Under optimal conditions hydrolysis (as measured by loss of optical density) was observed with purified *M. luteus* and *B. subtilis* cell walls but not with *S. aureus*, *S. mutans*, *E. faecalis*, or *L. arabinosus* (results not shown). The optimal specific activity of the purified enzyme was 450 U mg^{-1} using *B. subtilis* vegetative cell walls as substrate.

Determination of LytG Hydrolytic Bond Specificity. *B. subtilis* 1A304 purified peptidoglycan was hydrolyzed with purified LytG under conditions which resulted in <5% loss of OD_{450} and the soluble material was analyzed (Figure 4B). Two major peaks were observed (peaks 4 and 5, Figure 4B) which did not correspond to any of the previously characterized major Cellosyl derived muropeptides (Figure 4A). The novel products were collected, desalted, and analyzed by mass spectroscopy. On desalting it was observed that peak 5 consisted of two muropeptides. Both of these (called muropeptides 5 (1) and 5 (2)) were collected and analyzed by mass spectroscopy and amino acid analysis (Table 2). This identified these three muropeptides as disaccharide tripeptide (muropeptide 4) and disaccharide tripeptide disaccharide tetrapeptide (muropeptides 5(1) and 5(2)). However, the muropeptide elution pattern from HPLC shows that these muropeptides have different retention times than their equivalents observed by Atrih et al. (*35*) after muramidase (Cellosyl) digestion. This difference could be accounted for by the relative position of glucosamine residues. To determine the structures of these muropeptides, NMR analysis was performed. One-dimensional spectra were typical of muropeptides. In particular, the spectrum of muropeptide 5(1) (Figure 5a) contained two signals between 7.0 and 7.5 ppm, with intensities corresponding to single protons, indicating that 5(1) has a single amidation on one of the two available A_2pm residues. By contrast, the spectrum of 5(2) (data not shown) indicates two amidations, one on each A_2pm residue. The spectrum of muropeptide 5(1) (Figure 5a) has two prominent intense peaks at 2.04 and 2.11 ppm. We have previously shown (*35*) that these can be assigned to the acetyl methyls of MurNAc and GlcNAc, respectively, and do not

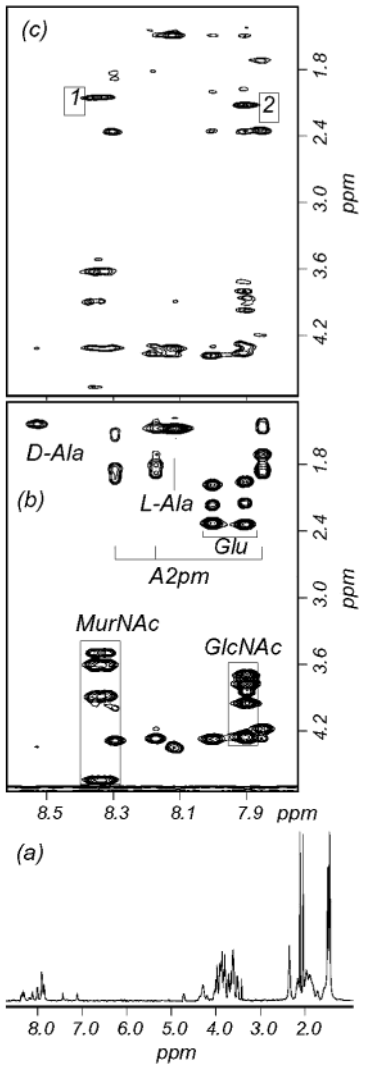

FIGURE 5: 500 MHz NMR spectra of muropeptide 5(1). Spectra were acquired in water containing 10% D_2O at 35 °C. (a) 1D spectrum. The water resonance was suppressed by presaturation and has been removed by a low-frequency digital convolution filter. (b) Part of the 2D TOCSY spectrum, indicating spin system assignments. The A_2pm signals correspond to correlations with both the α and δ amides. Correlations involving the sugar resonances are boxed. (c) Part of the 2D ROESY spectrum, same spectral region as part (b). The cross-peaks marked *1* and *2* are discussed in the text.

Table 2: Muropeptide Characterization

Muropeptide	Mass spectroscopy Ion	Observed *m/z*	Muropeptide composition Glc	Mur	Ala	Glu	A_2pm	Identity	Structure
1	$[M - H]^-$	665.4	0	1	1	1	1	Muramic acid tripeptide	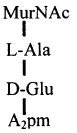
2	$[M - H]^-$	1,384.5	0	2	3	2	2	Monosaccharide tripeptide monosaccharide tetrapeptide	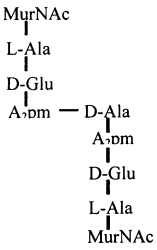
3	$[M - H]^-$	1,587.6	1	2	3	2	2	Disaccharide tripeptide disaccharide tetrapeptide with two amidations and missing one glucosamine	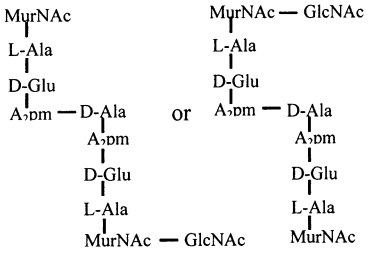
4	$[M + H]^+$	893.5	1	1	1	1	1	Disaccharide tripeptide with one amidation	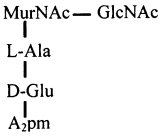
5 (1)	$[M + H]^+$	1,792.9	2	2	3	2	2	Disaccharide tripeptide disaccharide tetrapeptide with one (5(1)) or two (5(2)) amidations	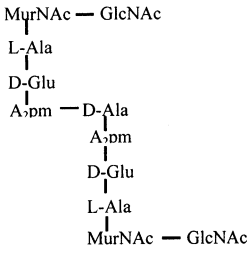
5 (2)	$[M + H]^+$	1,793.1	2	2	3	2	2		

change position significantly on reduction of the reducing end sugar.

The structures of the muropeptides were determined using 2D COSY, TOCSY, and rotating frame NOE (ROESY) spectra, and the method is illustrated using spectra of muropeptide 5(1) (Figure 5). The spin systems are clearly identifiable from TOCSY spectra (Figure 5b), which indicate for example two closely similar sets of sugar resonances coupled to 2′-amide protons at around 8.35 ppm (left-hand box in Figure 5b), and two more sets coupled to amide protons at around 7.9 ppm (right-hand box in Figure 5b). The chemical shifts indicate that the sets around 8.35 ppm retain characteristic pyranose sugar frequencies (in particular, the anomeric proton at around 4.7 ppm), while the sets around 7.9 ppm are from the reduced alcohol, i.e., this sugar is the reducing end. However, the chemical shift values are not sufficiently diagnostic to allow us to say with confidence which resonances come from MurNAc and which from GlcNAc. This assignment is made most unambiguously from the ROESY spectrum (Figure 5c) which contains intense cross-peaks (labeled 1 and 2), respectively from the MurNAc and GlcNAc 2′-amide proton to its adjacent acetyl methyl. This demonstrates that the reducing end is GlcNAc. Other sequential NOEs confirm the expected disaccharide tripeptide disaccharide tetrapeptide structure.

After partial hydrolysis of *B. subtilis* 1A304 peptidoglycan with LytG as above, total material was further hydrolyzed by Cellosyl, which resulted in >95% loss of OD_{450}, and the soluble products were analyzed by HPLC. Two apparently novel muropeptides (2 and 3) were observed in the LytG and Cellosyl digested material (Figure 4C) compared with the Cellosyl control (Figure 4A), and a large increase in peak

1 was also noted (Figure 4C). Muropeptides 1, 2, and 3 (Figure 4C) were collected, desalted, and analyzed by mass spectroscopy and amino acid analysis (Table 2). Muropeptides 1, 2, and 3 (Figure 4C) are muramic acid tripeptide, monosaccharide tripeptide monosaccharide tetrapeptide, and disaccharide tripeptide disaccharide tetrapeptide missing one glucosamine, respectively (Table 2). For muropeptide 3 the monosaccharide may be substituted with either the tri- or tetrapeptide side chain.

A digestion time course also failed to reveal any muropeptides other than disaccharides (muropeptides 4 and 5). Also Cellosyl digestion of soluble LytG products did not give any products apart from muropeptides 1, 2, and 3 (results not shown).

DISCUSSION

Sequence homology had suggested that LytG may be a muramidase (*25*). Thus, it was surprising that lack of LytG resulted in the disappearance of muropeptides from the *B. subtilis* 168 peptidoglycan profile that corresponded to those which had been previously predicted to be due to glucosaminidase activity, as a result of the lack of an *N*-acetylglucosamine residue at the nonreducing terminus (*35*). In contrast, missing the major, well characterized glucosaminidase, LytD, did not affect the muropeptide profile. Thus, it was proposed that LytG may be a glucosaminidase and constitutes the major activity of this type involved in peptidoglycan hydrolysis in the intact cell, even though it is not a major cell wall protein. The lack of LytD products may be due to the absence of appropriate substrate for this enzyme and stringent posttranslational control of activity. Despite intense speculation the biochemical regulation of autolysins in situ which prevents spontaneous autolysis has remained elusive. Very recently it has been shown that the cell wall of *B. subtilis* is protonated during growth (*37*). Both LytD and LytG have slightly acid pH optima, which suggests they may well be active in the cell wall environment.

To verify the hydrolytic bond specificity of LytG, the protein was overexpressed and purified. Muropeptide analysis of LytG hydrolyzed peptidoglycan revealed unequivocally that LytG is a glucosaminidase (Table 2 and Figure 4). Cellosyl (muramidase) digestion of LytG hydrolyzed peptidoglycan results in the loss of muropeptides 4 and 5 (Figure 4B) and the appearance of 1, 2, and 3 (Figure 4C). Thus muropeptides 4 and 5 are glucosaminidase-derived substrates for the muramidase. Muropeptide 4 is hydrolyzed by Cellosyl to produce muropeptide 1. Muropeptides 5(1) and 5(2) are muramidase hydrolyzed to make muropeptides 2 and 3, respectively, as revealed by their relative amidation status (Table 2). This confirms that LytG is a novel glucosaminidase unrelated to previous enzymes of this class. The homology of LytG to AcmA suggests that either related enzymes may have different activities or that previous methodologies used to determine hydrolytic bond specificity have not been stringent enough. Thus, it is important to verify activity using the sensitive RP-HPLC assay.

The presence of muropeptide 3 (which retains an *N*-acetylglucosamine residue) suggests that Cellosyl is unable to fully hydrolyze muropeptide 5(2). Muropeptide 2 was shown to have only one amidation by NMR, while muropeptide 3 had two amidations (Table 2). A conformational change, or steric hindrance, due to the presence of two amidations, may prevent the action of Cellosyl on both potential cleavage sites in 5(2). Thus, the amidation state effects peptidoglycan hydrolase activity. This may form a novel mode of posttranslational regulation of peptidoglycan hydrolase activity via this subtle modification of the stem peptide.

Hydrolysis of peptidoglycan with LytG alone resulted in the appearance of only disaccharide containing muropeptides (Figure 4B). These were monomer and dimer muropeptides. All three contained only disaccharide substitutions. Larger muropeptides were never recovered in significant quantities. Thus LytG is, at least primarily, an exoenzyme acting processively from the ends of the glycan strands. This is the first autolytic exo-glucosaminidase to be described in *B. subtilis* 168. The enzyme was able to efficiently hydrolyze only cell wall peptidoglycan from *B. subtilis* and *M. luteus* but not *S. aureus* and other species, which may be due to different substrate chemical structures. *O*-Acetylation of muramic residues in *S. aureus* may be responsible for this lack of activity, which has also been shown to prevent the hydrolysis of *S. aureus* peptidoglycan by lysozyme (*38*). Also, HF treatment of *B. subtilis* cell walls led to an increase in peptidoglycan hydrolysis rate by LytG. Teichoic acid and membrane phospholipids have previously been proposed to have moderating effects on LytD activity (*8*).

LytG is a new member of the family of vegetative autolysins of *B. subtilis* (*25*). These enzymes perform, in many cases, overlapping and mutually compensatory roles in multiple physiological functions. A number of autolysins have been shown to be involved in separation of daughter cells after septation (*6*, *39*). LytC, LytD, and LytG are all involved in boli formation (probably due to hyperfilamentation), as only the triple mutant forms such large clumps. Such levels of functional redundancy may be the result of the importance of cell separation in the natural environment and the presence of the autolysins in the exposed location of the cell wall open to attack by proteases etc. LytG also plays a role in motility and chemotaxis, as evidenced by a defect in swarming ability. This could be due to slight changes in filamentation status, which would impact on chemotactic ability, or flagellar extrusion may be effected by aberrant cell wall hydrolysis. Lysis due to azide or cell wall antibiotics occurs as a post-mortem event. In this case LytG and LytD showed mutually compensatory roles.

Transcriptional fusion and primer extension analysis revealed *lytG* transcription to occur from a single promoter, similar to the consensus sequence typical of σ^A-dependent promoters (*40*). This is in contrast to *lytC* and *lytD*, which are completely or in part under the control of the alternative sigma factor σ^D. Thus, LytG may have its primary function during exponential growth. The roles of the large complement of seemingly compensatory autolysins during growth and the mechanisms whereby all these components combine to create a functional cell wall architecture have remained obscure. The classical representation of peptidoglycan is as long glycan strands cross-linked periodically by peptide side chains. However evidence from *Escherichia coli* (*41*) and recently from *S. aureus* (*42*) have revealed this convention to be misleading. The average glycan strand length in *S. aureus* is in fact 6 disaccharides. Thus, the bulk of the peptidoglycan is made up of short chains, which must be

highly cross-linked in order to maintain integrity. The presence of oligomer muropeptides linking multiple chains alludes to a specific organization within the peptidoglycan. The accurate chain length of peptidoglycan of *B. subtilis* has not yet been determined. The activity of glucosaminidases, such as LytG and LytD, will be to modify glycan strand length. Their role in this crucial parameter for peptidoglycan structure is currently under investigation.

REFERENCES

1. Ghuysen, J.-M., Tipper, D. J., and Strominger, J. L. (1966) *Methods Enzymol. 8*, 685−699.
2. Rogers, H. J., Thurman, P. F., and Burdett, I. D. J. (1983) *J Gen. Microbiol. 129*, 465−478.
3. Fein, J. E., and Rogers, H. J. (1976) *J. Bacteriol. 127*, 1427−1442.
4. Fein, J. E. (1979) *J. Bacteriol. 137*, 933−946.
5. Pooley, H. M., and Karamata, D. (1984) *J. Bacteriol. 160*, 1123−1129.
6. Ward, J. B., and Williamson, R. (1984) in *Microbial Cell Wall Synthesis and Autolysis* (Nombela, C., Ed.) pp 159−166, Elsevier, Amsterdam.
7. Herbold, D. R., and Glaser, L. (1975) *J. Biol. Chem. 250*, 1676−1682.
8. Rogers, H. J., Taylor, C., Rayter, S., and Ward, J. B. (1984) *J. Gen. Microbiol. 130*, 2395−2402.
9. Kuroda, A., and Sekiguchi J. (1991) *J. Bacteriol. 173*, 7304−7312.
10. Lazarevic, V., Margot, P., Soldo, B., and Karamata, D. (1992) *J. Gen. Microbiol. 138*, 1949−1961.
11. Margot, P., and Karamata, D. (1992) *Mol. Gen. Genet. 232*, 359−366.
12. Margot, P., Mauël, C., and Karamata, D. (1994) *Mol. Microbiol. 12*, 535−545.
13. Blackman, S. A., Smith, T. J., and Foster, S. J. (1998) *Microbiol. 144*, 73−82.
14. Helmann, J. D., Marquez, L. M., and Chamberlin, M. J. (1988) *J. Bacteriol. 170*, 1568−1574.
15. Rashid, M. H. Mori, M., & Sekiguchi, J. (1995) *Microbiology 141*, 2391−2404.
16. Ortiz, J. M., Gillespie, J. B., and Berkeley, R. C. W. (1972) *Biochim. Biophys. Acta 289*, 174−186.
17. Berkeley, R. C. W., Brewer, S. J., Ortiz, J. M., and Gillespie, J. B. (1973) *Biochim. Biophys. Acta 309*, 157−168.
18. Brewer, S. J., and Berkeley, R. C. W. (1973) *Biochem. J. 134*, 271−281.
19. Ortiz, J. M., Berkeley, R. C. W., and Brewer, S. J. (1973) *J. Gen. Microbiol. 77*, 331−337.
20. Ortiz, J. M. (1974) *J. Bacteriol. 117*, 909−910.
21. Foster, S. J. (1992) *J. Bacteriol. 174*, 464−470.
22. Margot, P., Wahlen, M., Gholamhuseinian, A., Piggot, P., and Karamata, D. (1998) *J. Bacteriol. 180*, 749−752.
23. Ishikawa, S., Hara, Y., Ohnishi, R., and Sekiguchi, J. (1998) *J. Bacteriol. 180*, 2549−2555.
24. Margot, P., Pagni, M., and Karamata, D. (1999) *Microbiology 145*, 57−65.
25. Smith, T. J., Blackman, S. A., and Foster, S. J. (2000) *Microbiology 146*, 249−262.
26. Kunst, F., Ogasawara, N., Moszer, I., and 148 other authors (1997) *Nature 390*, 249−256.
27. Vagner, V., Dervyn, E., and Ehrlich, S. D. (1998) *Microbiology 144*, 3097−3104.
28. Sambrook, J., Fritsch, E. F., and Maniatis, T. (1989) *Molecular Cloning: a Laboratory Manual*, 2nd ed., Cold Spring Harbor Laboratory, Cold Spring Harbor, NY.
29. Guérout-Fleury, A.-M., Shazand, K., Frandsen, N., and Stragier, P. (1995) *Gene 167*, 335−336.
30. Hanahan, D. (1983) *Mol. Biol. 166*, 557−580.
31. Anagnostopoulos, C, and Spizizen, J. (1961) *J. Bacteriol. 81*, 741−746.
32. Sterlini, J. M., and Mandelstam, J. (1969) *Biochem. J. 113*, 29−37.
33. Laemmli, U. K. (1970) *Nature 227*, 680−685.
34. Horsburgh, M. J., and Moir, A. (1999) *Mol. Microbiol. 32*, 41−50.
35. Atrih, A., Bacher, G., Allmaier, G., Williamson, M. P., and Foster, S. J. (1999) *J. Bacteriol. 181*, 3956−3966.
36. Atrih, A., Zöllner, P., Allmaier, G., Williamson, M. P., and Foster, S. J. (1998) *J Bacteriol. 180*, 4603−4612.
37. Calamati, H. G., Ehringer, W. D., Koch, A. L., and Doyle, R. J. (2001) *Proc. Natl. Acad. Sci U.S.A. 98*, 15260−15263.
38. Snowden, M. A., Perkins, H. R., Wyke, A. W., Hayes, M. V., and Ward, J. B. (1989) *Microbiology 135*, 3015−3022.
39. Forsberg, C., and Rogers, H. J. (1971) *Nature 229*, 272−273.
40. Haldenwang, W. G. (1995) *Microbiol. Rev. 59*, 1−30.
41. Harz, H., Burgdorf, K., and Holtje, J.-V. (1990) *Anal. Biochem. 190*, 120−128.
42. Boneca, I. G., Huang, Z.-H., Gage, D., and Tomasz, A. (2000) *J. Biol. Chem. 275*, 9910−9918.

BI020498C